

# Development of gold thin-film for optical-based biosensor

Cite as: AIP Conference Proceedings **2230**, 020008 (2020); <https://doi.org/10.1063/5.0006687>  
Published Online: 04 May 2020

Teguh Handoyo, and Jun Kondoh



View Online



Export Citation

## ARTICLES YOU MAY BE INTERESTED IN

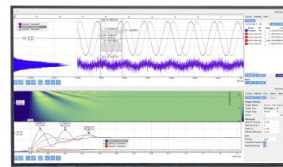
[Extended and localized surface plasmons in annealed Au films on glass substrates](#)  
Journal of Applied Physics **108**, 074303 (2010); <https://doi.org/10.1063/1.3485825>

[Effects of Annealing on Thin Gold Films](#)  
Journal of Applied Physics **37**, 2085 (1966); <https://doi.org/10.1063/1.1708676>

[The effect of acetate additives on inoculum on VS, COD and microbial communities on food waste anaerobic digestion](#)  
AIP Conference Proceedings **2230**, 020004 (2020); <https://doi.org/10.1063/5.0003725>

## Challenge us.

What are your needs for  
periodic signal detection?



Zurich  
Instruments

# Development of Gold Thin-Film for Optical-based Biosensor

Teguh Handoyo<sup>1, 2, a)</sup> and Jun Kondoh<sup>1, 3, b)</sup>

<sup>1</sup>*Graduate School of Science and Technology (GSST), Shizuoka University, 3-5-1 Johoku, Naka-ku, Hamamatsu-shi, Shizuoka 432-8561, Japan*

<sup>2</sup>*Badan Pengkajian dan Penerapan Teknologi (BPPT), Gedung Teknologi 3 No. 254, Kawasan PUSPITEK, Serpong, Tangerang 15314 Indonesia*

<sup>3</sup>*Graduate School of Integrated Science and Technology (GSIST), Shizuoka University, 3-5-1 Johoku, Naka-ku, Hamamatsu-shi, Shizuoka 432-8561, Japan*

<sup>a)</sup>Corresponding author: teguh.handoyo.17@shizuoka.ac.jp

<sup>b)</sup>kondoh.jun@shizuoka.ac.jp

**Abstract.** The localized surface plasmon resonance phenomenon of gold (Au) nanostructured in thin film form has many attractiveness for optical based sensing applications. Plasmon resonance robustly influences optical properties the Au thin film. Therefore, the optical response of Au thin film determined by nanostructure of Au nanoparticles on the surface of substrate. However, the thermal annealing strongly affects to the nanostructure Au thin film. In this study, low-cost Au thin film has been developed by vacuum thermal evaporation technique and thermal annealing process. The thermal annealing was applied in certain temperature 400 °C with various annealing durations were applied to generate Au thin-films. The effect of thermal annealing on nanostructure and optical properties of Au thin films were measured. The statistical quantities of the average height value of grain particles was between 13 to 21 nm and the density was between 100 to 200 particles per square micrometer after annealing. The optical properties of gold thin-film in terms to be applied as sensor in optical-based biosensor reported. The best of RIS sensitivity obtained above 90 nm RIU-1. The results appearance a great promising for sensor applications.

## INTRODUCTION

Over the past few decades, research in the localized surface plasmon resonance (LSPR) phenomenon on metal nanomaterials has been contributing the evolution of optical sensing platforms that less-expensive, rapid detection, significant sensitivity, and provide for miniaturization in order to point-of-care needs. Gold (Au) nanomaterials have been considerably used in various electrochemical and optical sensor applications for signal enhancement (1). In addition, Au is the most non-reactive of all metals and is favorable in all natural and industrial environments. Moreover, Au as a noble metal is very attractive and superior than other metals due to its withstanding to corrosion in moist air, which means it will not rust or tarnish, resistance to oxidation, and catalytic characteristics, which are strongly linked with its electronic structure (2).

Au nanomaterials due to their sensitivity to structure, size, and shape are applied widely in sensor systems for spectroscopy of LSPR which is highly determined by changing the film nanostructure and morphology of the material (3) and surrounding medium refractive index (4). In other hand, optical-based sensor such as optofluidic can be coupling with LSPR sensors supported gold nanoparticles (AuNPs). Theoretically, LSPR is a phenomenon of the collective oscillation of electrons at the interface of metallic structures which the size of the interface much smaller than the incident wavelength in specialized condition (5). It can open the way for the opportunities for integrated optical-based biosensor with LSPR sensor for many analytical and biological applications.

There have been several experimental reports for fabrication of metal nanoparticles for thin film, which contain small amounts of material, which means it is low-cost in material source. Several techniques to fabricate nanometallic thin film such as vacuum thermal evaporation, colloidal synthesis, electron beam lithography (EBL), nanosphere lithography (NSL), NSL with reactive ion etching (RIE) and focused ion beam lithography (FIBL). One

of the simplest and economics to fabricate Au thin films correlated to other techniques is a vacuum thermal evaporation technique (6). In addition to growth the formation of the AuNPs on glass substrates to conduct thin film, thermal annealing process is often used to achieve a structure thermodynamically more stable (7). Furthermore, we propose Au thin film as LSPR sensors were fabricated by the vacuum thermal evaporation method and thermal annealing process with various annealing duration.

In this work, the topography of the Au thin films obtained by vacuum thermal evaporation method and thermal annealing process with various annealing duration was investigated. This work has been performed in order to demonstrate the potential of obtained thin-film for optical-based biosensor applications, the refractive index sensitivity (RIS) determined experimentally measurement absorbance spectra by surrounding medium with different refractive index.

## METHODS AND EXPERIMENTS

### Fabrication of Au thin films

Fig. 1 gives an overview of the fabrication process of the Au thin films of our experiments. The Au thin films were fabricated using the vacuum thermal evaporation method. Firstly, the glass substrate with thickness 0.17~0.25 mm (Micro cover glass No. 2, 18 mm x 18 mm size, Matsunami Glass Ind., Japan) were cleansed thoroughly with acetone ((CH<sub>3</sub>)<sub>2</sub>CO) and 2-propanol (CH<sub>3</sub>CHOHCH<sub>3</sub>) solution (Wako Pure Chemical Industries Ltd., Japan). Details of the cleansing and deposition method are described as in previous our report (8). Au thin-film A, B and C were made using pure Au materials 5.4 mg. The distance between an evaporation material source and a glass substrate was  $140 \pm 1$  mm.

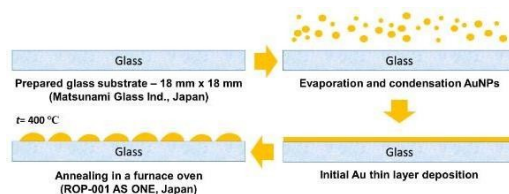


**FIGURE 1.** Schematic illustration of workflow for fabrication Au thin films with vacuum thermal evaporation followed by thermal annealing at 400 °C

The thermal annealing was applied with a furnace oven (Model ROP 001, AS One, Japan) to create AuNPs on the glass surface. The Au thin-films were thermally annealed at temperature 400 °C in uncontrolled atmospheric conditions. The duration of annealing for each thin-film A, B and C were 8 hours, 24 hours and 36 hours, respectively. Post annealing process, all Au thin-films naturally cooled down.

### Characterization of Au thin-films

The topography of Au thin-films measured by atomic force microscopy (AFM) SPA-400 (SII Hitachi, Japan) at Center for Instrumental Analysis in Hamamatsu Campus, Shizuoka University. All AFM images were acquired in non-contact scanning mode for  $2.2 \mu\text{m} \times 2.2 \mu\text{m}$ . For AFM images data evaluation, the Gwyddion 2.49 software was used. The optical properties of AuNPs films were determined spectrally at wavelengths of 350 - 1000 nm using an USB4000 UV-Vis spectrophotometer (Ocean Optics, Inc USA) with halogen light source device (Model: 5-2300, Soma Optics, Ltd Japan) in room temperature. The sensitivity of Au thin-film was obtained with a various of liquid (water, ethanol and oil) as medium with different refractive indices. Schematic experimental setup in this work was shown in Fig. 2.

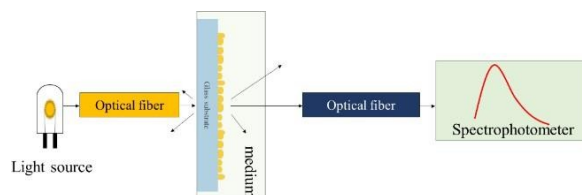


**FIGURE 2.** Schematic experimental setup for optical properties measurement

## RESULTS AND DISCUSSION

### Topography of Films and Grain Particles

Au thin-films were deposited on glass substrate using a vacuum thermal evaporation equipment. The nominal average thickness of the thin-films is estimated as 1.13 nm by the distance between the glass substrate from the evaporation metal source. The topography of Au thin-films fabricated were investigated by AFM with non-contact scanning mode (dynamic force microscope-DFM). The DFM mode prevent scraping or degradation effects by cantilever on occasional Au thin films observed after doing multiple scans compare with contact scanning mode. Accordingly, in this work, it decided to measure the surface of the Au thin films layer. In particular, an AFM scan was achieved and surface topography images were provided together with a rough surface of the thin-film. The obtained AFM images data were evaluated using freeware Gwyddion 2.49. In view of this work, the grain statistics were used to estimate the AuNPs size distribution on glass substrate (9). The initial Au thin films before annealing were fabricated in same batch fabricating by vacuum thermal evaporation, so that it can be compared with the Au thin films after annealing. Fig. 3 represents 2D surface morphology AFM images of Au thin films A, B and C before annealing. As can be seen in Figure 3, the Au thin films surface structure was unclearly. Fig. 4 represents 2D and 3D surface topography AFM images of Au thin films after thermal annealing at 400 °C in various duration annealing for thin-film A, B and C were 8 hours, 24 hours, respectively. Comparing to Fig. 4, the Au thin films surface structure was changed after thermal annealing process.

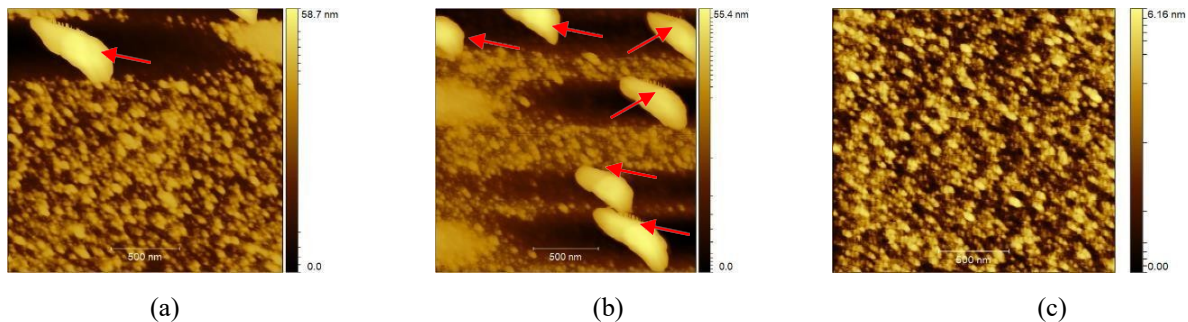


**FIGURE 3** 2D AFM images of Au thin films before annealing by freeware Gwyddion 2.49. The scale bars are 500 nm long. (a) Au thin film A, (b) Au thin film B, and (c) Au thin film C. For (a) and (b), there are dust (red arrows) on the surface of Au thin film A and Au thin film B, respectively, and the dust size is the length of about 500nm and the width of about 200nm. For (c), the maximum height of the roughness is 6.16 nm. In this case, (a), (b) and (c) show no clear base structure of AuNPs deposited on the Au thin films

Although, in this study, the annealing temperature is lower than the relatively melting point of bulk Au (1064 °C), but it was acceptably significant to cause initial Au thin films layer deposited on glass substrate were melting and change the structure of Au thin films on glass substrate. It should be recognized that, for nanosize materials, their melting point was decrease to be lower than their melting point of bulk material. In addition, these images also demonstrate the resulting size and shape of the nanoparticle on the glass substrate after annealing at 400 °C was homogenous almost rounded, although significant deviation occurred in nanoscale. Moreover, this results also demonstrate that the nanostructure formation of the surface of Au thin-film could be affected by the annealing treatment.

Accordingly, the time duration and temperature of the annealing treatment caused surface diffusion mechanism which due to a devaluation of the surface energy of the Au thin-film and the interface energy between the glass substrate and the Au thin-film (10). The Au atoms obtain higher kinetic energy and mobility to aggregate with each other to generate AuNPs (2). The small nanoparticles size will concatenate to form bigger nanoparticles size (11). Indeed, the initial thickness of AuNP layer could lead affect the results of nanoparticles size on surface glass substrate.

The statistical analysis measurement of average equivalent disc diameter of grain particles, number of grain particle distributions, average height value, and average roughness (Ra) of the surface thin films by Gwyddion 2.49 software were summarized in Table 1. Table 1 presents that the nanoparticle size before and after annealing is

smaller than the incident wavelength used in this work (350–1000 nm). Thus, it will meet the physically requirements for the occurrence of LSPR spectra on the Au thin-film. This result also explains experimentally that the annealing process made the structure of the before annealing film changes. Hence, temperature and time duration of annealing affect on the average height value and the average roughness of the thin-film increases, see in Fig. 5.

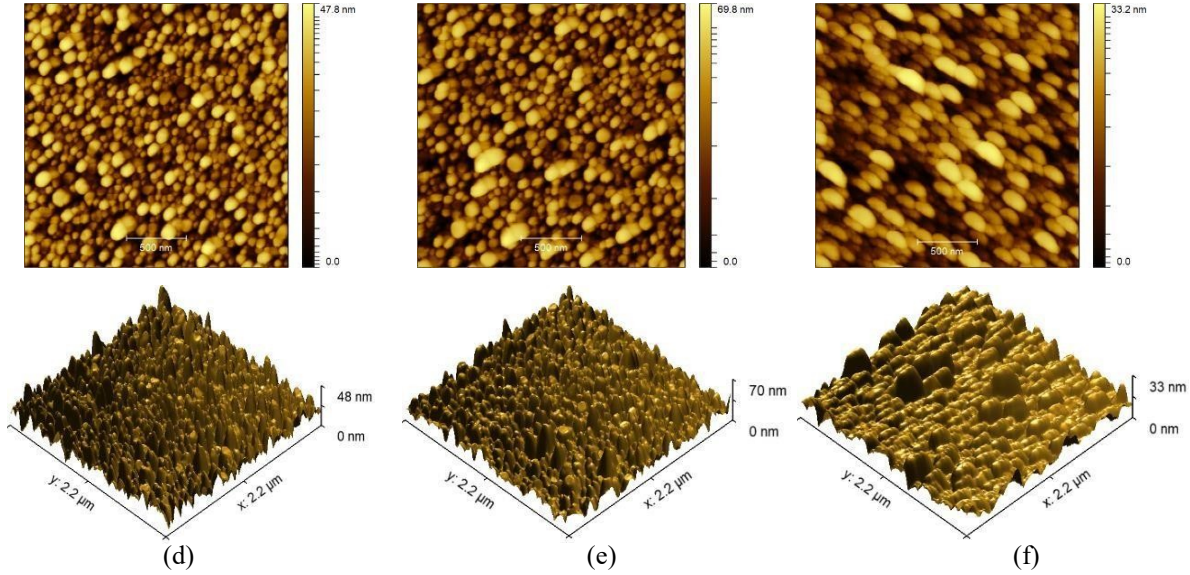


**FIGURE 4** (a), (b) and (c) are 2D AFM images of Au thin films A, B and C after annealing at 400 °C, respectively. The scale bars are 500 nm long. The maximum height of the roughness for Au thin films A, B and C after annealing at 400 °C are 47.8 nm, 69.8 nm and 33.2 nm, respectively. (d), (e) and (f) are 3D AFM images of Au thin films A, B and C after annealing, respectively. Scan area 2.2 μm x 2.2 μm

A histogram of the equivalent disc diameter size distributions of AuNP grain particles on the surface of thin-films can be seen in Fig. 6. The histogram shows a change in the distribution of equivalent disc diameter grain particles. As we can see more than 94% of the equivalent disc diameter of Au grains particles after annealing is less than or equal to 50 nm. Moreover, it can be understood that the agglomeration between particles occurs while the annealing was done. In addition, the glass substrate is a common substrate for Au thin-film based LSPR sensors, providing less expensive and transparent, which is favorable for transmission-based spectroscopy in the visible to near-IR range spectrum. Nonetheless, the insufficient adhesion of AuNP on glass substrate could be solved with annealing process and the process can improve the stability of Au thin-film (12).

**TABLE 1.** Statistical analysis measurement of au thin films (scan area 2 μm x 2 μm)

|  | Au thin-film A | Au thin-film B | Au thin-film C |
|--|----------------|----------------|----------------|
| Time duration of annealing (hours)               | 8              | 24             | 36             |
| Number of grain particles (per μm <sup>2</sup> ) |                |                |                |
| <i>Before-annealing</i>                          | 154            | 140            | 355            |
| <i>After annealing</i>                           | 194            | 156            | 107            |
| Average equivalent disc diameter of grain (nm)   |                |                |                |
| <i>Before-annealing</i>                          | 22.98          | 17.39          | 13.87          |
| <i>After annealing</i>                           | 17.14          | 15.35          | 18.43          |
| Average roughness (R <sub>a</sub> )              |                |                |                |
| <i>Before-annealing</i>                          | 2.450          | 5.042          | 0.432          |
| <i>After annealing</i>                           | 4.942          | 6.251          | 3.259          |
| Average height value (nm)                        |                |                |                |
| <i>Before-annealing</i>                          | 11.60          | 14.50          | 2.837          |
| <i>After-annealing</i>                           | 21.74          | 24.33          | 13.36          |

## Optical response and sensitivity measurement

Optical response and sensitivity were measured in wavelengths between 350 to 1000 nm. The dependence absorbance and sensitivity of all thin-films were investigated as shown in Fig. 7 and Fig. 8. Measuring the absorbance was done by measuring the intensity of light pass through the Au thin film by comparison the initial light intensity reaching the Au thin films on glass substrate using the spectrophotometer. Fig. 7 shows the LSPR spectra of Au thin-film before and after annealing on dry measurement and as we can see the interference occurred. In optics, if light is incident on a metal thin-film of refractive index ( $n_f$ ), assembled onto a glass substrate of refractive index ( $n_{gs}$ ), then at the air-thin-film, the thin-film-glass substrate and the glass substrate-air interfaces, part of the incident intensity is reflected and part of it is transmitted. Thus, since the reflected and transmitted beams originate from a single light source, the beams will exhibit interference effects (13).

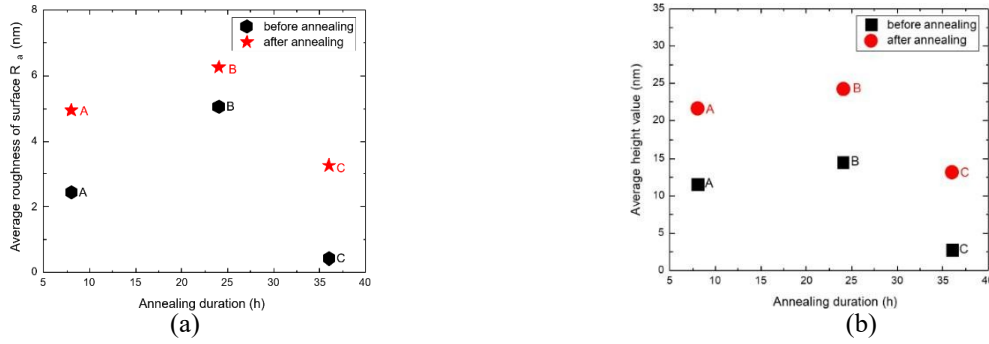


**FIGURE 5** (a) Average roughness surface and (b) Average height value of Au thin-film A, B and C after annealing in various annealing duration: 8h, 24h and 36h, respectively

As shown in Fig. 7, the optimal wavelength for all thin-films after annealing process was about 560 nm. Indeed, this also explains why the natural color of the Au material was yellowish. The results should be noted that the temperature of annealing affects to absorbance spectra of all Au thin films after annealing compare to before annealing. In addition, another reason is LSPR spectral influenced by the optical constants of the thick thin-film (14).

Moreover, distribution of AuNPs or the interparticle gap might be affect significant changes in extinction spectra (15). By the decreasing nanogap distance, the electromagnetic enhancement rapidly increases because of an interparticle coupling and thus influences their optical response (16). Equation 1 following the Drude model, the bulk plasmon frequency  $\omega_p$  influenced by the free electron density  $N$  and on the effective mass  $m_e$  of the electron or optical mass which includes the coupling of the free electrons to the ion core (17). Following the Mie theory, the plasmon frequency depends on the dielectric functions of the surrounding medium and of the particle material.

$$\omega_p = \sqrt{\frac{Ne^2}{\epsilon_0 m_e}} \quad (1)$$

Absorbance spectra as shown in Fig. 7, it considered that the spectral peaks of Au thin-films before annealing were relatively broadened by multipolar excitations and radiative damping (18). It has been reported that the resonance peak wavelength influenced by the longitudinal-transverse mode (17). The annealing treatment on the fabrication of the Au thin-film was done in order to achieve the small width of the peak of LSPR spectra and it was desirable for sensing purpose (19) and also for Au thin-film stabilization (12).

To characterize the sensitivity of thin-films optically, we have used various mediums with disparate refractive indices, i.e.; air ( $n_{air}=1.00$ ), water ( $n_{water}=1.33$ ), ethanol ( $n_{ethanol}=1.36$ ) and oil ( $n_{oil}=1.47$ ). Experimentally, the RIS of obtained Au thin-film were summarized in Table 2. The shift of LSPR peak wavelength ( $\Delta\lambda_p$ ) is relatively linear with variation refractive index of the surrounding medium ( $\Delta n$ ). Accordingly, particularly the RIS is usually reported in number of wavelengths per refractive index unit (nm RIU<sup>-1</sup>) (18). Mathematically, it has been described

by the following Equation 2:

$$RIS = \Delta\lambda_p \Delta n \quad (2)$$

Figs. 8(a), 8(b), and 8(c) show the LSPR spectra of Au thin-film A, B, C with various mediums, respectively. In sequence, as shown in Fig. 8(d) and Fig. 8(e), the LSPR peak wavelength and the peak absorbance value increases with increasing value of the medium refractive index. In Figure 8(f) shows that RIS of Au thin films increases as the refractive index medium increases from  $n=1.33$  to  $n=1.47$  RIU.

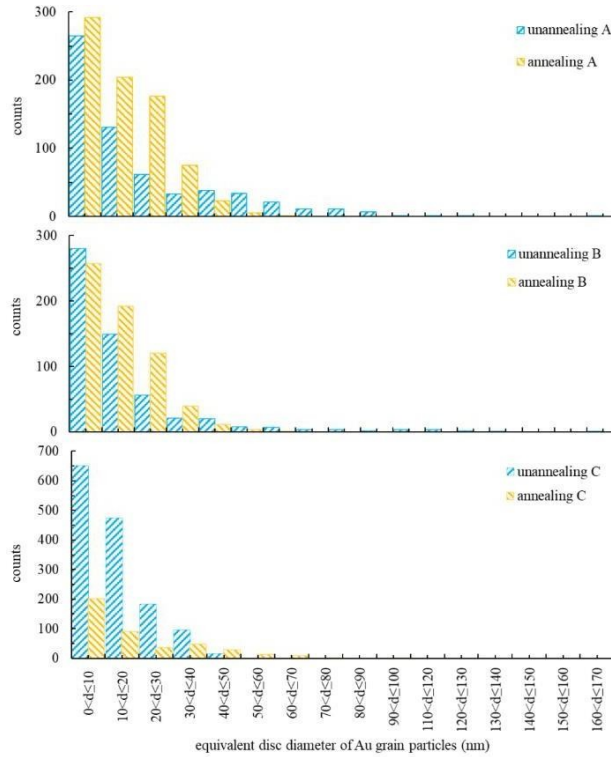


**FIGURE 6** Histogram of equivalent disc diameter of Au grain particles evaluated statistically on obtained Au thin-films A, B and C before and after thermal annealing process at 400 °C with annealing duration 8h, 24h and 36h, respectively

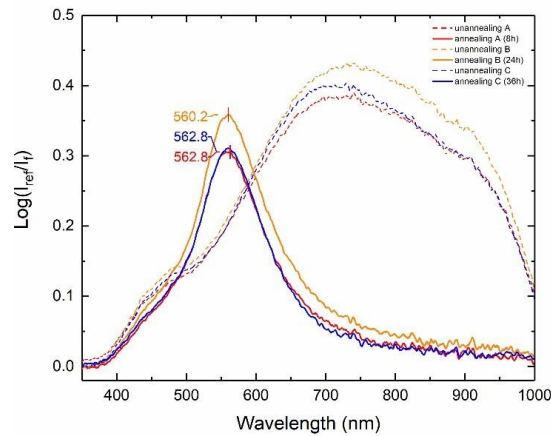


**FIGURE 7** The LSPR spectra absorbance of Au thin-film A, B, and C before and after thermal annealing on dry measurement. In this case, measured LSPR spectra for Au thin films A, B and C after annealing exhibit peaks located in wavelength at 562.8 nm, 562.8 nm and 560.2 nm, respectively

The obtained RIS value experimentally was not linear with increasing refractive index medium value ( $n$ ), especially for thin-film A and B for water and ethanol medium. However, RIS value generally was a significant difference with the difference in the medium refractive index value. We consider three possible reasons for this case. One, this occurred because of the formation in nanostructure of thin-films. In this case, including size, shape, and surface roughness on thin-film (5,20). Au nanospheres exhibit the smallest index sensitivity, and Au nano-branches exhibit the highest index sensitivity (21). Second, this happened because of the area sensing slightly shifted. Third, considered with Beer-Lambert's law, the thickness of the thin-film determines the LSPR spectra.

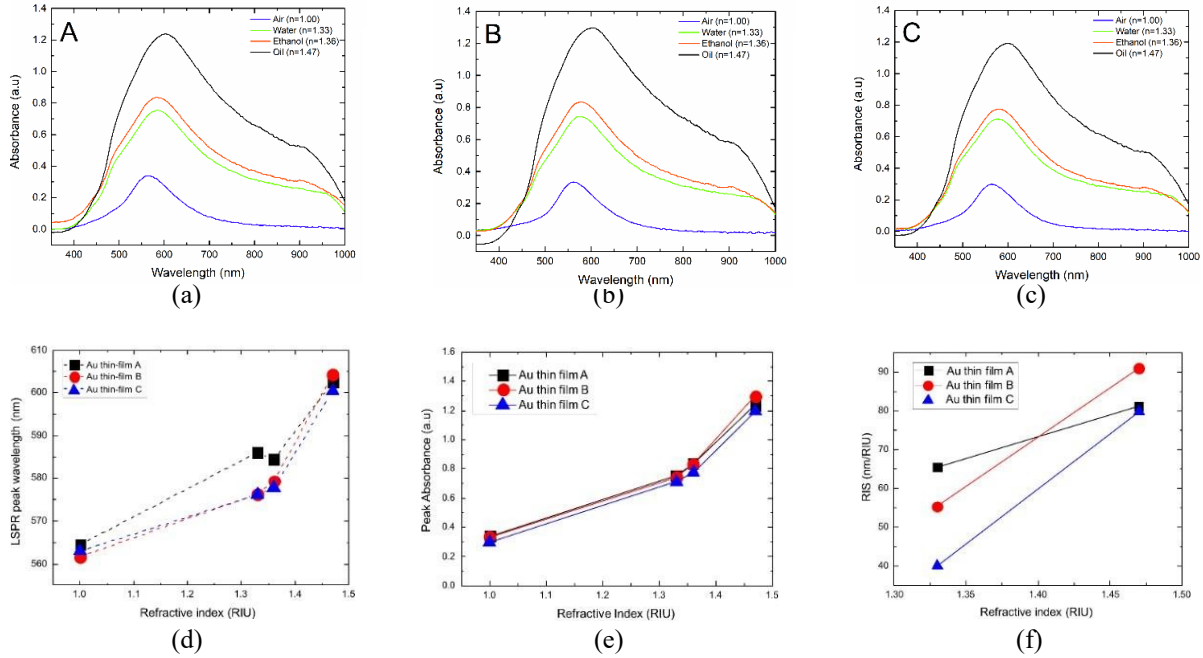


**FIGURE 8** (a), (b) and (c) are LSPR absorbance spectra of Au thin film A, B, and C measured in different liquid, respectively; (d) LSPR peak wavelength versus the refractive index; (e) Peak absorbance versus the refractive index; (f) The obtained RIS of Au thin-films versus the refractive index

Therefore, it is very important to regard with the structure of the thin film as sensor and to set the sensor on a fixed place. However, the results of RIS sensitivity, which obtained with Au thin-film B (above  $90 \text{ nm RIU}^{-1}$ ), is better than some of the published results with analogous technique (19). These results indicate that the transmission LSPR-based on Au thin-films in terms of the potential for optical-based biosensor applications.

## CONCLUSION

In this work, we developed and experimentally fabricated of Au thin-films by vacuum thermal evaporation followed by annealing process and investigated their properties. We have successfully demonstrated that the Au thin films could contribute a rationally sensitive in terms to be applied as optical based sensor. The size, shape and grain distribution influenced by annealing process are discussed. The numerical of refractive index sensitivity can be obtain up  $90 \text{ nm RIU}^{-1}$ . As one of the most significant challenges, our Au thin film as sensor open available a high potential for optical based biosensor.

## ACKNOWLEDGMENTS

The first authors acknowledge the financial support for Ph.D. study at Shizuoka University by Research and Innovation in Science and Technology Project (RISET Pro) Scholarship Program from Ministry of Research, Technology and Higher Education (RISTEKDIKTI), Republic of Indonesia. The authors appreciate the technical

support from all member of SWE (Surface Wave Electronic) Laboratory and Center for Instrumental Analysis in Hamamatsu Campus at Shizuoka University for their AFM technical support. Particularly, T. Handoyo also thanks to Mr. Hironori Sano for his assistance in thin-film fabrication and discussion.

## REFERENCES

1. Cao X, Ye Y, Liu S. Gold nanoparticle-based signal amplification for biosensing. *Anal Biochem [Internet]*. 2011;417(1):1–16. Available from: <http://dx.doi.org/10.1016/j.ab.2011.05.027>
2. Chan K, Goh BT, Rahman SA, Muhamad MR, Dee CF, Aspanut Z. Annealing effect on the structural and optical properties of embedded Au nanoparticles in silicon suboxide films. *Vacuum*. 2012;86(9):1367–72.
3. Emami M, Goodarzi R. Optoelectronic correlations for gold thin films in different annealing temperature. *Optik (Stuttg)*. 2018;171(April):397–403.
4. Noguez C. Surface plasmons on metal nanoparticles: The influence of shape and physical environment. *J Phys Chem C*. 2007;111(10):3606–19.
5. Willets KA, Van Duyne RP. Localized Surface Plasmon Resonance Spectroscopy and Sensing. *Annu Rev Phys Chem*. 2007;58(1):267–97.
6. Serrano A, De La Fuente OR, García MA. Extended and localized surface plasmons in annealed Au films on glass substrates. *J Appl Phys*. 2010;108(7).
7. Romanyuk VR, Kondratenko OS, Fursenko O V., Lytvyn OS, Zynyo SA, Korchovyi AA, et al. Thermally induced changes in thin gold films detected by polaritonic ellipsometry. *Mater Sci Eng B Solid-State Mater Adv Technol*. 2008;149(3):285–91.
8. Handoyo T, Kondoh J. Characterization of self-assembled AuNPs film for optofluidic applications. In: 2018 4th International Conference on Nano Electronics Research and Education (ICNERE) [Internet]. IEEE; 2019. p. 1–5. Available from: <https://ieeexplore.ieee.org/document/8642602>
9. Chicea D. Using AFM topography measurements in nanoparticle sizing. *Rom Reports Phys*. 2014;66(3):778–87.
10. Schmid G, Dellith J, Schneidewind H, Zopf D, Stranik O, Gawlik A, et al. Formation and characterization of silver nanoparticles embedded in optical transparent materials for plasmonic sensor surfaces. *Mater Sci Eng B Solid-State Mater Adv Technol*. 2015;193(C):207–16.
11. Bechelany M, Maeder X, Riesterer J, Hankache J, Lerosé D, Christiansen S, et al. Synthesis mechanisms of organized gold nanoparticles: Influence of annealing temperature and atmosphere. *Cryst Growth Des*. 2010;10(2):587–96.
12. Karakouz T, Maoz BM, Lando G, Vaskevich A, Rubinstein I. Stabilization of gold nanoparticle films on glass by thermal embedding. *ACS Appl Mater Interfaces*. 2011;3(4):978–87.
13. Manificier JC, Gasiot J, Fillard JP. A simple method for the determination of the optical constants n, k and the thickness of a weakly absorbing thin film. *Journal of Phys E Sci Instruments*. 1976;9:1002–4.
14. Kovalenko S, Fedorovych R. Optical properties of thin gold film. *Semicond Physics, Quantum Electron Optoelectron*. 2000;(1):383–8.
15. Guo L, Jackman JA, Yang HH, Chen P, Cho NJ, Kim DH. Strategies for enhancing the sensitivity of plasmonic nanosensors. *Nano Today [Internet]*. 2015;10(2):213–39. Available from: <http://dx.doi.org/10.1016/j.nantod.2015.02.007>
16. Xu H. *Nanophotonics Manipulating Light with Plasmons*. Pan Stanford Publishing Pte. Ltd. 2018.
17. Link S, Wang ZL, El-Sayed MA. Alloy formation of gold-silver nanoparticles and the dependence of the plasmon absorption on their composition. *J Phys Chem B*. 1999;103(18):3529–33.
18. Mayer KM, Hafner JH. Localization Surface Plasmon Resonance. *Chem Soc Rev [Internet]*. 2009;8(SUPPL. 2):435–7. Available from: <https://pubs.acs.org/sharingguidelines>
19. Bonyar A, Wimmer B, Csarnovics I. Development of a localised surface plasmon resonance sensor based on gold nanoparticles. *Proc 2014 37th Int Spring Semin Electron Technol ISSE 2014*. 2014;369–74.
20. Lumdee C, Yun B, Kik PG. Effect of surface roughness on substrate-tuned gold nanoparticle gap plasmon resonances. *Nanoscale*. 2015;7(9):4250–5.
21. Chen H, Kou X, Yang Z, Ni W, Wang J. Shape- and size-dependent refractive index sensitivity of gold nanoparticles. *Langmuir*. 2008;24(10):5233–7.